ARTICLE   OPEN

Quantum non-Gaussian multiphoton light

Ivo Straka [1], Lukáš Lachman[1], Josef Hloušek [1], Martina Miková[1], Michal Mičuda[1], Miroslav Ježek [1] and Radim Filip[1]

We propose an experimental method of recognizing quantum non-Gaussian multiphoton states. This is a native quantum property of Fock states, the fundamental quantum states with a constant number of particles. Our method allows experimental development and characterization of higher Fock states of light, reaching even beyond the current technical limits of their generation. We experimentally demonstrate that it is capable of distinguishing realistic quantum non-Gaussian light with the mean number of photons up to five despite detection efficiency of 50%. We also provide evidence that our method can help to distinguish the number of single-photon emitters based only on their collective emission.

INTRODUCTION

Over the past few years, generation of multiphoton nonclassical states of light became important for quantum technology.[1,2] Their unique feature is that they represent a bundle of indistinguishable photons with pronounced particle behavior. This behavior is altogether incompatible with any semi-classical continuous optical waves.[3–6] Many recent experimental steps brought us closer to generating Fock states $|n\rangle$ of light, essential resources with a fixed and constant number of photons n.[7–9] In our discussion, we focus on the quantum aspects of Fock states. Some of them are very susceptible to optical losses.[10,11] Namely, the negative regions in their Wigner quasiprobability density are very sensitive even for ideal noiseless states.[12] Consequently, Fock states of light have been experimentally approached only up to $|3\rangle$ in terms of this negativity.[8,9] On the other hand, nonclassical light can be produced rather easily for much higher number of photons by squeezing or conditioning.[13,14] Apparently, there is a large unexplored extension of multiphoton nonclassical states toward high Fock states of light.

Exploring this large extension of nonclassical states is a challenging task, on both theoretical and experimental side. However, quantum technology is boosting this ongoing investigation. A distinct step into the large gap between nonclassical states and Fock states was done when a criterion for single-photon quantum non-Gaussian (QNG) light was proposed.[15] Analogously to the definition of nonclassical light, QNG state cannot be expressed as *any probabilistic mixture of Gaussian states*. That covers all possible sources available from linearized quantum dynamics of light. More QNG criteria utilizing phase-space quasiprobability distributions have been proposed.[16–19] Experimental verification was done using both single-photon detectors and homodyne detection.[20–25] Single-photons were tested for robustness up to 20 dB of optical attenuation. Moreover, QNG has unique properties that have been explored in detail for single-photon states. Among these properties are dependence on optical loss[22] and a positive upper bound on the Wigner function at zero.[16] These two properties represent a significant distinguishment from both nonclassicality and Wigner function negativity, opening up a new class of multiphoton quantum states.

Recently, quantum non-Gaussianity of light has been proposed as a test bed for optical links suitable for quantum key distribution,[26] as opposed to the photon autocorrelation function that is typically measured. However, this single criterion[20] cannot be efficiently applied to all multiphoton states. For example, even ideal multiphoton Fock states $|2\rangle$ to $|6\rangle$, when attenuated below the respective transmittances $\eta = 0.30, 0.42, 0.50, 0.53, 0.63$, cannot be detected as QNG light using the single-photon criterion.[27] These ideal states are, however, QNG regardless of the attenuation, so such criteria should exist.

Here, we consider commonly available multichannel detectors and derive the QNG criteria precisely for them, and experimentally verify QNG multi-mode light up to nine heralded photons (see Results) despite collection and detection loss of 50%. Although these states are apparently sub-Poissonian, our approach to QNG is not related to the photon-number variance, but to experimental indivisibility of n photons. This fundamental particle property limits the probability of all $n + 1$ channels in the detector firing at once. This can be measured directly and does not require reconstruction or tomography of any kind. We can further estimate the robustness of multiphoton states of light under optical loss unavoidable in potential applications. The resulting loss tolerance is quantified as QNG depth, defined as the maximum optical attenuation applicable on a specific quantum state, after which the QNG can still be witnessed.

The key contribution of our proposed approach is to development of experimental multiphoton states toward ideal Fock states, as QNG represents a necessary milestone along the way, interposing between nonclassicality and Wigner function negativity. It also provides a physical measure of robustness—QNG depth—directly as a result. Therefore, it serves both as QNG witness and quantifies the maximum tolerable optical loss.

RESULTS

Multi-photon QNG criteria

A suitable case to consider is a multichannel detector, as it is widely available in many laboratories.[28–30] The detector splits incoming light to multiple separate single-photon binary
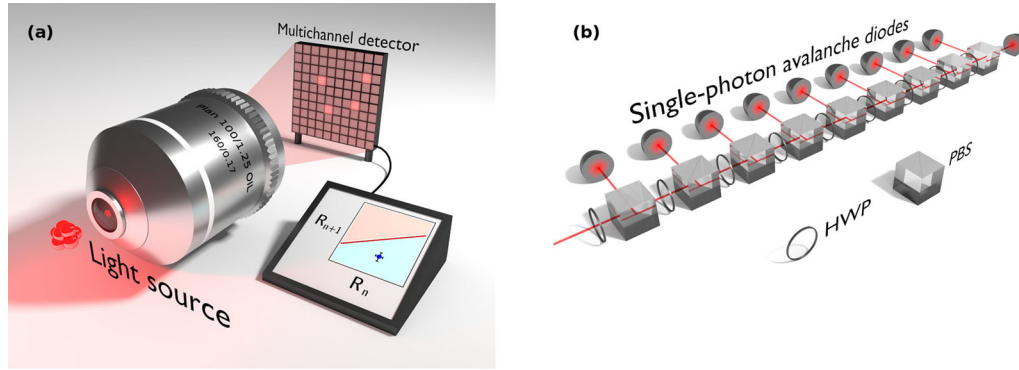
Fig. 1 A general proposal of the experimental QNG witness. **a** Multi-photon light is collected and brought to a balanced multichannel detector, where coincidences R_n, R_{n+1} are compared to the QNG threshold. **b** The detector in our experiment consists of ten silicon single-photon avalanche diodes (SPAD) and a balanced array of polarizing beam splitters (PBS) and half-wave plates (HWP) to control the splitting ratio. The half-wave plates can be adjusted to split the light equally to any number of selected channels, so there is no need to physically add or remove SPADs

detectors, as depicted in Fig. 1. We consider only detection probabilities denoted as R_n and R_{n+1} for the detector with $n + 1$ identical channels. First, we choose n particular channels, then R_n is the probability of successful detection on these, irrespectively to the state of the odd channel. R_{n+1} is the probability of all $n + 1$ channels registering photons. Thus, we will be directly witnessing whether the measured $R_{n,n+1}$ are incompatible with any mixture of Gaussian states of light. Such detection technique is not sensitive to phase properties of light and can also be applied to multi-mode structures of light. Therefore, it is suitable for testing a wide range of optical sources.

We consider a linear functional

$$F(a) = R_n + aR_{n+1} \tag{1}$$

where a is a free parameter. Since $R_{n,n+1}$ are linear functions of quantum states and their photodistributions, for a given a, there is a maximum $F_{max}(a)$ that can be reached among mixtures of Gaussian states; that is squeezed coherent states.[15] Then, for given measured values of $R_{n,n+1}$, we get the function $F_{meas}(a)$. If there exists any a_0, for which the maximum of Gaussian mixtures is surpassed, $F_{meas}(a_0) > F_{max}(a_0)$, the measured state is QNG.

Since (1) is a linear functional of the quantum state of light, the maximum F_{max} is reached for a pure Gaussian state.[15,31] However, each mode is still parametrized by the maximal amplitude of displacement, minimal quadrature variance and a phase shift between them. The resulting minimum threshold for R_n as a function of R_{n+1} is a highly nonlinear function of three parameters per mode. For single-mode light, precise numerical solution is possible. The details of derivation are given in Methods and the Supplementary Material. For multi-mode light, the number of parameters increases, so we used Monte-Carlo simulations to find the thresholds. As is shown in Supplementary Material, the multi-mode thresholds are identical to the single-mode thresholds.

For light with small mean number of photons, the thresholds can be approximated by a useful analytical formula

$$R_n^{n+2} > H_n^4(x) \left[\frac{R_{n+1}}{2(n+1)^3} \right]^n, \tag{2}$$

where $H_n(x)$ is the maximum value of a Hermite polynomial among such $x : H_{n+1}(x) = 0$. Derivation is presented in the Supplementary Material where a more precise approximation is also derived.

Experimental results

Experimentally, it is very challenging to generate a multi-photon quantum state that would be sufficiently close to a Fock state.

Previous efforts have succeeded in generating heralded sub-Poissonian states with a high mean-photon-number.[13,32–34] However, QNG requires much more than sub-Poissonian light. For such heralded states, the main issue are systematic high-photon-number contributions coupled with optical loss in the trigger channel. The overall efficiency required to generate QNG light would have to be very close to 100% and thus beyond current technical capabilities. Multi-mode states allow us to overcome these limitations, and still the same QNG criteria apply–if the measurement gives a certain detection statistic, the QNG criterion gives identical results regardless of the number of modes measured. Using this correspondence in detection statistic, we produced QNG multi-mode states to show that the proposed criteria can indeed recognize corresponding single-mode states. Such single-mode states would represent the missing link on the way toward Fock states, between nonclassicality and Wigner function negativity.

To achieve this, we produced multi-photon states by mixing n single-photon states together incoherently using time multiplexing. As an additional advantage, this approach simulates incoherent mixing of signals from a cluster of n identical single-photon emitters in separate modes. This is a very relevant topic, because recognizing nonclassical properties of such clusters or simply counting these emitters is subject to ongoing research, which offers limited accuracy.[35–39]

In our experimental set-up, we used a collinear type-II spontaneous parametric down-conversion in a periodically poled KTP crystal, which was pumped by a narrow-band continuous-wave laser diode at 405 nm. We already showed that such sources generate very high-quality heralded single-photon states.[22] We took n successive time windows, where a single-photon was heralded, and joined them into a single temporal detection unit. Due to this approach and exceptional brightness and efficiency of the source, we were able to generate a photon statistics exhibiting QNG and proved it for n up to 9 (Fig. 2, for more details, see Methods/Supplementary Material).

As a multichannel detector, we constructed a network of polarizing beam splitters (PBS) and half-wave plates to facilitate a balanced 1-to-$(n + 1)$ splitter. The design is equivalent to the one depicted in Fig. 1b, but we used a tree structure instead of a linear one. In each arm, a silicon single-photon avalanche diode (SPAD) was placed as a detector. Even though each SPAD has different efficiency, it is sufficient to adjust the PBS network so that the responses of all detectors are balanced. This way, the measured state is merely subjected to additional loss, but that does not create any false positives in QNG witnessing.[20] The total number
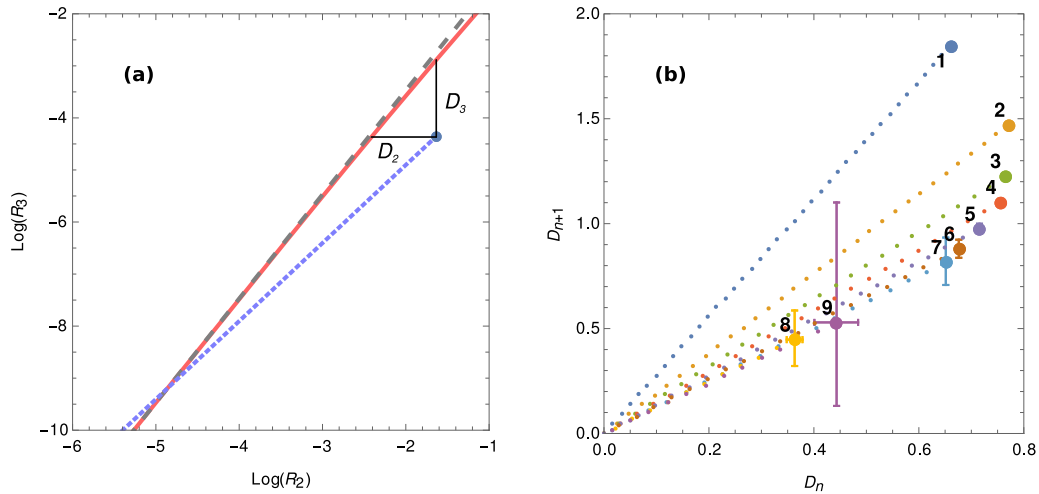
Fig. 2 QNG tests for heralded 1–9 photons. **a** Example for $n = 2$. Red line represents the QNG criterion, while dashed gray line is its approximation (2). The blue point represents the measured state and the dotted blue line is the path of the point if the state becomes further attenuated. For the sake of visualizing all data, we denote D_n, D_{n+1} as the horizontal and vertical log-distances between a measured point and the QNG threshold. **b** The distances D_n and D_{n+1} for generated n-photon states were measured on a balanced $(n + 1)$-channel detector (numbered points for $n = 1 - 9$). Reaching the point of origin at zero means that QNG is no longer recognizable. Dotted paths represent attenuation with steps of 0.5 dB. Note that these steps are not the same size for all n. The number of steps on each path is proportional to QNG depth. For QNG depth values, see Fig. 3. Both vertical and horizontal error bars are shown for all data points; in some cases they are smaller than point size. For individual depiction of each multiphoton state with its respective QNG criterion, see Fig. 2 in the Supplementary Material

of detection ports was ten on the measured state and one for the heralding detector.

We estimate the mean numbers of photons to be up to five, if we take into account the detector efficiency that was ≈50%. However, no correction has been done in the data, and our results represent direct witnessing of QNG using a lossy detector. In this regime, witnessing the negativity of the Wigner function would not be possible.

The measured states are very robust against optical loss, withstanding up to 5–20 dB of attenuation before their QNG character becomes undetectable. In previous work, we demonstrated that this QNG depth can be precisely predicted.[22]

In Fig. 3, QNG depths of various multi-photon states are shown, as measured using multiple QNG criteria. Here, each multi-photon state is positively detected with at least one order of the QNG criterion.

DISCUSSION

Let us discuss an insight into the behavior of the QNG criteria. As per Eq. 2 and shown in Fig. 2, the QNG borders are approximately linear on a log–log scale with a slope of $(n + 2)/n$, the approximation being low mean number of photons. Attenuation paths behave similarly with a slope of $(n + 1)/n$, assuming low realistic noise in the sense of fast-decaying photodistribution of the measured state $P_n \gg P_{n+1} \gg \sum_{k=n+2}^{\infty} P_k$. Because the QNG slope is always greater, the two dependencies eventually intersect and quantum states have typically some finite QNG depth. The robustness observed in our data is due to low multiphoton contributions in our single-photon states. When combining n of them, the photodistribution becomes almost binomial with a weak systematic noise, $P_{\leq n} \gg P_{>n}$, and consequently, $R_n \gg R_{n+1}$ for experimental rates. This sharp contrast is necessary for QNG and was the reason for our choice of using multi-mode heralded single-photon states.

Generally, if the criterion order is lower than the number of merged single-photons (white area in Fig. 3), the dominant contributions to R_n, R_{n+1} arise from probabilities of heralded
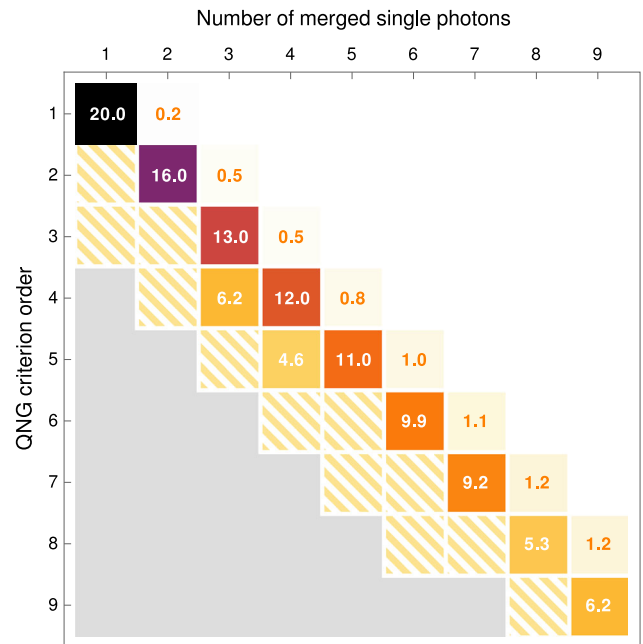

Fig. 3 Table of QNG depths (in dB), defined as the maximum attenuation, for which the quantum state is still QNG. The horizontal axis shows the number of single-photon states that comprise the measured state. The vertical axis represents the order of the QNG criterion used to measure the state (n in Eq. 1). The diagonal represents the data being shown in Fig. 2. Solid-colored tiles represent points with positively measured QNG despite statistical uncertainties. For points above the diagonal, the depth estimates are conservative and lower than the actual QNG depth, because R_{n+1} is no longer caused solely by noise. The upper white region represents combinations of measured states and criteria that did not show QNG. Orange stripes denote measurements where statistical uncertainty intersects with the QNG criterion border, making the result inconclusive. Data in the gray region contain no detections at all

generation of n, $n+1$ photons, respectively. These results have a very low uncertainty, but mostly fail to pass the QNG criterion; chiefly due to optical loss.[27] If the criterion order is higher than the number of single-photons, these coincidences are always caused by noise with very low detection rates. Those cases are mostly inconclusive, unless measured for excessively longer periods of time. In between, there is always an optimal criterion that recognizes QNG for the widest range of potential optical loss (the diagonal in Fig. 3).

This complies well with our initial motivation to test the indivisibility of n photons using a criterion with $n+1$ detectors. Practically, if we consider the measured quantum states as a simulated collective emission from n identical single-photon emitters, these optima offer a potential way to count the emitters based only on their emission. This hypothesis would heavily depend on the quality of the single-photon emitters, but our data show that, at least in our simulation, QNG depth is capable of accurate distinction for a high number of emitters. Current methodology for counting or resolving individual single-photon emitters also uses multichannel detectors, but has limited accuracy. Results have been published for fluorescent dye molecules[35–37] and for quantum dots.[38,39] We hope future measurements will explore this approach further using emission from physical samples.

In this work, we introduced and verified an experimental approach to direct witnessing of QNG multi-photon states as a necessary step toward multi-photon Fock states. This method is capable of recognizing multi-photon states produced by multiple atoms or molecules, trapped ions or solid-state emitters, that can or cannot be individually controlled.[35] When investigating a cluster of single-photon emitters, the collectively emitted light can be detected as QNG before any single emitter is isolated or controlled. We also demonstrated that these measurements are feasible with realistic detection efficiency. Moreover, this method is generally applicable to quantum states of matter producing QNG states of light, for example, in quantum optomechanics.[40]

METHODS

Experiment

We used an emission from multiple heralded single-photon states temporally merged together. The single-photon source uses a collinear type-II spontaneous parametric down-conversion in a 6-mm thick ppKTP crystal and poling period 10 μm. As a pump, we used a narrow-band continuous-wave laser diode at 405 nm. The heralding rate was set to about 650 kHz, which corresponds to the maximum data flow allowed by the coincidence electronics. The spectral bandwidth of the photons is about 1 nm full width at half maximum and the Hong-Ou-Mandel uncorrected visibility 98%. The raw heralding efficiency was about 30%.

The temporal merging of n single-photons was achieved by considering a number of consecutive coincidence time windows as parts of one temporal detection mode. The positions of these respective time windows were heralded by a detector in one of the SPDC modes. This is equivalent to collecting light from n independent single-photon emitters in n modes. The criteria for R_n, R_{n+1} for n modes can be verified to be identical to the case of $n=1$ using the Monte-Carlo approach. Additionally, the detection statistics of this state is the same as for a single-mode state with equivalent photodistribution. This only requires that all SPADs work in binary mode. To achieve this, if a SPAD registers detections in multiple coincidence windows that are part of one detection mode, it is considered as a single detection only.

For detection, we used two time-to-digital converters, each having eight channels with the resolution of 81 ps/time bin. Since we needed 11 channels in total, we used two modules and synchronized them with a shared periodic signal at 100 kHz. This frequency was chosen to compensate the measured relative clock drift 10^5 time bins/s.

Statistical methods. Error bars in Fig. 2 denote minimum-width Bayesian confidence intervals (68%) assuming a uniform prior. The reason for this

was that the primary source of statistical uncertainty was a discrete counting process, where measured values were as low as one count.

QNG criterion

In Eq. 1, we defined a general linear functional of coincidence probabilities $R_{n,n+1}$

$$F(a) = R_n + aR_{n+1}. \tag{3}$$

Now we show the maximization of $F(a)$ over pure Gaussian states.

The probabilities $R_{n,n+1}$ are best expressed using a probability of vacuum in an attenuated state,

$$P_0(\tau) = Tr\left[(|0\rangle\langle 0| \otimes \mathbb{1}) \cdot U(\tau) \cdot (\rho \otimes |0\rangle\langle 0|) \cdot U(\tau)^\dagger\right], \tag{4}$$

where ρ is the density matrix of the state and $U(\tau)$ is a unitary operator corresponding to a beam splitter with transparency τ. The probability of n simultaneous detections on given channels—R_n—is obtained by a summation

$$R_n = 1 + \sum_{k=1}^{n} (-1)^k \binom{n}{k} P_0(k/N), \tag{5}$$

where N is the total number of spatial modes, which the detector can distinguish. The identity (5) implies that the probability (4) determines the probability R_n. For a pure Gaussian state (4) reads

$$P_0(\tau) = 2 \frac{e^{-\frac{\beta^2 \tau}{2}\left[\frac{\cos^2 \phi}{\mu(1/V)} + \frac{\sin^2 \phi}{\mu(V)}\right]}}{\sqrt{\mu(V)\mu(1/V)}}, \tag{6}$$

where

$$\begin{aligned} \beta e^{i\phi} &= \frac{1+V}{2\sqrt{V}}a + \frac{1-V}{2\sqrt{V}}a^*, \\ \mu(V) &= 2V + \tau(1-V) \end{aligned} \tag{7}$$

with β real and positive. The parameter a denotes a complex amplitude of a coherent state, which undergoes quadrature squeezing and V is the minimal quadrature variance in time.

The expressions (5) and (6) give raise to the linear combination of probabilities for a pure Gaussian state

$$F_{a,n}(\beta, V, \phi) = R_n + aR_{n+1}. \tag{8}$$

Thus, the optimizing task is well parametrized and can be done numerically. It has turned out that the global maximum requires $\phi = 0$ for each a and order n. The remaining two parameters fulfill a necessary condition of a local extreme

$$\partial_\beta R_n \partial_V R_{n+1} = \partial_V R_n \partial_\beta R_{n+1}. \tag{9}$$

It ensues from the exclusion of the a parameter from the equations giving conditions on a local extreme. Although this relation does not specify a, it leads to the solution of the problem, when the task is understood equivalently as optimization of the probability of success R_n over the set of states with a constraint on error probability R_{n+1} and Lagrange multiplier a. The resulting maximal success probability is bound to the error probability only by a single parameter determined by the relation (9).

Data availability

The data that support the findings of this study are available from the corresponding author upon request.

AUTHOR CONTRIBUTIONS

L.L. and R.F. derived the QNG criteria and provided the theoretical analysis. I.S. built the SPDC source and performed the measurement and data analysis. J.H. built the multichannel detector. M.J., M. Miková, and M. Mičuda participated in the experimental work. M.J. closely supervised and coordinated the experiment. I.S., R. F., and L.L. wrote the manuscript and all authors were involved in creating and revising the manuscript. R.F. initiated and coordinated the project.

ADDITIONAL INFORMATION

Supplementary information accompanies the paper on the *npj Quantum Information* website (https://doi.org/10.1038/s41534-017-0054-y).

Competing interests: The authors declare no competing financial interests.

Publisher's note: Springer Nature remains neutral with regard to jurisdictional claims in published maps and institutional affiliations.

REFERENCES

1. Holland, M. J. & Burnett, K. Interferometric detection of optical phase shifts at the heisenberg limit. *Phys. Rev. Lett.* **71**, 1355–1358 (1993).
2. Pan, J. -W., Bouwmeester, D., Daniell, M., Weinfurter, H. & Zeilinger, A. Experimental test of quantum nonlocality in three-photon greenberger-horne-zeilinger entanglement. *Nature* **403**, 515–519 (2000).
3. Wang, X. -B., Hiroshima, T., Tomita, A. & Hayashi, M. Quantum information with gaussian states. *Phys. Rep.* **448**, 1–111 (2007).
4. Braunstein, S. L. & van Loock, P. Quantum information with continuous variables. *Rev. Mod. Phys.* **77**, 513–577 (2005).
5. Ferraro, A., Olivares, S. & Paris, M. G. A. *Gaussian States in Quantum Information*. (Bibliopolis, Napoli, 2005).
6. Weedbrook, C. et al. Gaussian quantum information. *Rev. Mod. Phys.* **84**, 621–669 (2012).
7. Bimbard, E., Jain, N., MacRae, A. & I., L. Quantum-optical state engineering up to the two-photon level. *Nat. Photon-*. **4**, 243–247 (2010).
8. Cooper, M., Wright, L. J., Söller, C. & Smith, B. J. Experimental generation of multi-photon fock states. *Opt. Express* **21**, 5309–5317 (2013).
9. Yukawa, M. et al. Generating superposition of up-to three photons for continuous variable quantum information processing. *Opt. Express* **21**, 5529–5535 (2013).
10. Yurke, B. & Stoler, D. Measurement of amplitude probability distributions for photon-number-operator eigenstates. *Phys. Rev. A* **36**, 1955–1958 (1987).
11. Rubin, M. A. & Kaushik, S. Loss-induced limits to phase measurement precision with maximally entangled states. *Phys. Rev. A* **75**, 053805 (2007).
12. Zurek, W. H. Decoherence, einselection, and the quantum origins of the classical. *Rev. Mod. Phys.* **75**, 715–775 (2003).
13. Harder, G. et al. Single-mode parametric-down-conversion states with 50 photons as a source for mesoscopic quantum optics. *Phys. Rev. Lett.* **116**, 143601 (2016).
14. Iskhakov, T. S., Pérez, A. M., Spasibko, K. Y., Chekhova, M. V. & Leuchs, G. Superbunched bright squeezed vacuum state. *Opt. Lett.* **37**, 1919–1921 (2012).
15. Filip, R. & Mišta, L. Detecting quantum states with a positive wigner function beyond mixtures of gaussian states. *Phys. Rev. Lett.* **106**, 200401 (2011).
16. Genoni, M. G. et al. Detecting quantum non-gaussianity via the wigner function. *Phys. Rev. A* **87**, 062104 (2013).
17. Hughes, C., Genoni, M. G., Tufarelli, T., Paris, M. G. A. & Kim, M. S. Quantum non-gaussianity witnesses in phase space. *Phys. Rev. A* **90**, 013810 (2014).
18. Park, J. et al. Testing nonclassicality and non-gaussianity in phase space. *Phys. Rev. Lett.* **114**, 190402 (2015).
19. Park, J. et al. Revealing nonclassicality beyond gaussian states via a single marginal distribution. *Proc. Natl. Acad. Sci.* **114**, 891–896 (2017).
20. Ježek, M. et al. Experimental test of the quantum non-gaussian character of a heralded single-photon state. *Phys. Rev. Lett.* **107**, 213602 (2011).
21. Predojević, A. et al. Efficiency vs. multi-photon contribution test for quantum dots. *Opt. Express* **22**, 4789–4798 (2014).
22. Straka, I. et al. Quantum non-gaussian depth of single-photon states. *Phys. Rev. Lett.* **113**, 223603 (2014).
23. Ježek, M. et al. Experimental test of the strongly nonclassical character of a noisy squeezed single-photon state. *Phys. Rev. A* **86**, 043813 (2012).
24. Baune, C., Schönbeck, A., Samblowski, A., Fiurášek, J. & Schnabel, R. Quantum non-gaussianity of frequency up-converted single photons. *Opt. Express* **22**, 22808–22816 (2014).
25. Song, H., Kuntz, K. B. & Huntington, E. H. Limitations on the quantum non-gaussian characteristic of schrödinger kitten state generation. *New J. Phys.* **15**, 023042 (2013).
26. Lasota, M., Filip, R. & Usenko, V. C. Robustness of quantum key distribution with discrete and continuous variables to channel noise. *ArXiv e-prints*, 1602.03122 (2016).
27. Lachman, L. & Filip, R. Quantum non-gaussianity from a large ensemble of single photon emitters. *Opt. Express* **24**, 27352–27359 (2016).
28. Achilles, D., Silberhorn, C., Śliwa, C., Banaszek, K. & Walmsley, I. A. Fiber-assisted detection with photon number resolution. *Opt. Lett.* **28**, 2387–2389 (2003).
29. Fitch, M. J., Jacobs, B. C., Pittman, T. B. & Franson, J. D. Photon-number resolution using time-multiplexed single-photon detectors. *Phys. Rev. A* **68**, 043814 (2003).
30. Lundeen, J. S. et al. Tomography of quantum detectors. *Nat. Phys.* **5**, 27–30 (2009).
31. Lachman, L. & Filip, R. Robustness of quantum nonclassicality and non-gaussianity of single-photon states in attenuating channels. *Phys. Rev. A* **88**, 063841 (2013).
32. O'Sullivan, M. N., Chan, K. W. C., Lakshminarayanan, V. & Boyd, R. W. Conditional preparation of states containing a definite number of photons. *Phys. Rev. A* **77**, 023804 (2008).
33. Laurat, J., Coudreau, T., Treps, N., Matre, A. & Fabre, C. Conditional preparation of a quantum state in the continuous variable regime: Generation of a sub-poissonian state from twin beams. *Phys. Rev. Lett.* **91**, 213601 (2003).
34. Iskhakov, T. S. et al. Heralded source of bright multi-mode mesoscopic sub-poissonian light. *Opt. Lett.* **41**, 2149–2152 (2016).
35. Weston, K. D. et al. Measuring the number of independent emitters in single-molecule fluorescence images and trajectories using coincident photons. *Anal. Chem.* **74**, 5342–5349 (2002).
36. Kurz, A. et al. Counting fluorescent dye molecules on dna origami by means of photon statistics. *Small* **9**, 4061–4068 (2013).
37. Ta, H. et al. Mapping molecules in scanning far-field fluorescence nanoscopy. *Nat. Commun.* **6**, 7977 (2015).
38. Mangum, B. D., Ghosh, Y., Hollingsworth, J. A. & Htoon, H. Disentangling the effects of clustering and multi-exciton emission in second-order photon correlation experiments. *Opt. Express* **21**, 7419–7426 (2013).
39. Israel, Y., Tenne, R., Oron, D. & Silberberg, Y. Quantum correlation enhanced super-resolution localization microscopy enabled by a fibre bundle camera. *Nat. Commun.* **8**, 14786 (2017).
40. Riedinger, R. et al. Non-classical correlations between single photons and phonons from a mechanical oscillator. *Nature* **530**, 313–316 (2016).